Maintenance of chondroitin sulfation balance by chondroitin-4-sulfotransferase 1 is required for chondrocyte development and growth factor signaling during cartilage morphogenesis

Michael Klüppel[1], Thomas N. Wight[2], Christina Chan[2], Aleksander Hinek[3] and Jeffrey L. Wrana[1,*]

[1]Programme in Molecular Biology and Cancer, Samuel Lunenfeld Research Institute, Mount Sinai Hospital, 600 University Avenue, Toronto, Ontario M5G 1X5, Canada
[2]The Hope Heart Program, Benaroya Research Institute at Virginia Mason, 1124 Columbia Street, Seattle, WA 98104-2046, USA
[3]Division of Cardiovascular Research, The Hospital for Sick Children, Toronto, Ontario M5G 1X8, Canada
[4]Department of Molecular and Medical Genetics and Microbiology, University of Toronto, Toronto M5S 1A8, Canada
*Author for correspondence (e-mail: wrana@mshri.on.ca)

Accepted 20 June 2005

Development 132, 3989-4003
Published by The Company of Biologists 2005
doi:10.1242/dev.01948

Summary

Glycosaminoglycans (GAGs) such as heparan sulfate and chondroitin sulfate are polysaccharide chains that are attached to core proteins to form proteoglycans. The biosynthesis of GAGs is a multistep process that includes the attachment of sulfate groups to specific positions of the polysaccharide chains by sulfotransferases. Heparan-sulfate and heparan sulfate-sulfotransferases play important roles in growth factor signaling and animal development. However, the biological importance of chondroitin sulfation during mammalian development and growth factor signaling is poorly understood. We show that a gene trap mutation in the BMP-induced chondroitin-4-sulfotransferase 1 (*C4st1*) gene (also called carbohydrate sulfotransferase 11 – *Chst11*), which encodes an enzyme specific for the transfer of sulfate groups to the 4-O-position in chondroitin, causes severe chondrodysplasia characterized by a disorganized cartilage growth plate as well as specific alterations in the orientation of chondrocyte columns. This phenotype is associated with a chondroitin sulfation imbalance, mislocalization of chondroitin sulfate in the growth plate and an imbalance of apoptotic signals. Analysis of several growth factor signaling pathways that are important in cartilage growth plate development showed that the *C4st1*$^{gt/gt}$ mutation led to strong upregulation of TGFβ signaling with concomitant downregulation of BMP signaling, while Indian hedgehog (Ihh) signaling was unaffected. These results show that chondroitin 4-O-sulfation by C4st1 is required for proper chondroitin sulfate localization, modulation of distinct signaling pathways and cartilage growth plate morphogenesis. Our study demonstrates an important biological role of differential chondroitin sulfation in mammalian development.

Key words: Gene trapping, Chondroitin-4-sulfotransferase 1, Bone morphogenesis, Cartilage growth plate, Chondroitin sulfate spatial distribution, Osteoarthritis, Growth factor signaling, Chst11

Introduction

Glycosaminoglycans (GAGs) such as heparan sulfate (HS) and chondroitin sulfate (CS) are long chains of repeating disaccharide subunits, which are covalently linked to core proteins to form proteoglycans (Sugahara and Kitagawa, 2000). During the biosynthesis of GAGs in the Golgi, a number of sulfotransferases modify the disaccharide subunits and GAG chains through transfer of sulfate groups to specific positions on the sugar moieties (Habuchi, 2000; Kusche-Gullberg and Kjellen, 2003; Selleck, 2000; Sugahara and Kitagawa, 2000). Mature proteoglycans can be cell membrane-bound or are part of the extracellular matrix (ECM) and are important in a wide range of biological processes, including cell migration, proliferation and survival, as well as modulation of growth factor signaling (Kirn-Safran et al., 2004; Perrimon and Hacker, 2004; Selleck, 2000; Sugahara and Kitagawa, 2000).

Although the role of heparan sulfation in development and growth factor signaling has been extensively studied (Garcia-Garcia and Anderson, 2003; Grobe et al., 2002; Kirn-Safran et al., 2004; Koziel et al., 2004; Merry and Wilson, 2002; Nybakken and Perrimon, 2002; Perrimon and Hacker, 2004; Shworak et al., 2002; Wilson et al., 2002), the biological function of chondroitin sulfation is less well understood. During development and in disease, chondroitin sulfation on carbon positions 4 (C4S) and 6 (C6S) is tightly controlled both spatially and temporally (Kitagawa et al., 1997; Theocharis et al., 2003; Tsara et al., 2002). Furthermore, although deletion of mouse chondroitin-6-sulfotransferase 1 (*C6st-1*; *Chst3* – Mouse Genome Informatics) does not affect skeletal development, in humans, mutations in *C6ST1* (*CHST1*; Human Gene Nomenclature Database) are associated with chondrodysplasia (Thiele et al., 2004).

Most skeletal structures are formed by endochondral ossification, in which a transient cartilage template is replaced by bone. During cartilage morphogenesis, chondrocytes in the growth plate undergo a complex and highly regulated program

Development

of proliferation and differentiation (Karsenty and Wagner, 2002; Shum et al., 2003). The periarticular region of the growth plate contains a reservoir of immature resting as well as non-directionally proliferating chondrocytes. Subsequently, chondrocytes form a columnar layer by assuming a flattened cell shape and proliferate in stacks along the longitudinal axis of the developing bone. In the hypertrophic zone, chondrocytes terminally differentiate and elaborate a mineralized vascularized matrix that is then replaced by osteoblasts to generate primary bone (Karsenty and Wagner, 2002; Shum et al., 2003). By contrast, many cranial bones as well as the midshaft of long bones are formed directly by intramembraneous ossification without a cartilage intermediate (Karsenty and Wagner, 2002).

Several signaling pathways control the morphogenesis of the cartilage growth plate, including Ihh, parathyroid hormone-like peptide (Pthlp), fibroblast growth factor (FGF) and others. For example, the Ihh-Pthlp negative-feedback loop regulates the size of proliferative zone and the onset of hypertrophy (Vortkamp, 2001) and chondrocyte maturation is a complex, tightly regulated developmental process (Karsenty and Wagner, 2002; Shum et al., 2003; Vortkamp, 2001). Members of the transforming growth factor (TGFβ) family also play important roles during cartilage morphogenesis (Karsenty and Wagner, 2002; Klüppel et al., 2000; Serra and Chang, 2003). In particular, TGFβ1 promotes chondrogenesis in cultures of early undifferentiated mesenchyme, but inhibits both chondrocyte proliferation and hypertrophy in long bone organ cultures (Serra and Chang, 2003). Activating mutations in TGFβ1 have been identified in Camurati-Engelmann disease, which is characterized by a thickening of the bone collar of long bones (Campos-Xavier et al., 2001; Janssens et al., 2000; Janssens et al., 2003; Saito et al., 2001). Targeted deletion of the TGFβ2 gene results in alterations in size and shape of limb rudiments and bifurcation of the sternum (Sanford et al., 1997). In contrast, the TGFβ-related bone morphogenetic proteins (BMPs) positively regulate both chondrocyte proliferation and hypertrophy (Horiki et al., 2004; Yoon and Lyons, 2004). For example, mice with mutations in the BMP receptor type 1B develop brachydactyly (Baur et al., 2000; Yi et al., 2000), and mice overexpressing the negative regulators of BMP signaling, Smad6 and Smurf1, display delayed chondrocyte hypertrophy and dwarfism (Horiki et al., 2004). These studies establish that skeletal patterning and development are major targets for this morphogen superfamily (Klüppel et al., 2000; Rountree et al., 2004; Yoon and Lyons, 2004).

During an induction gene trap screen in ES cells and embryoid bodies for target genes of TGFβ and BMP signaling, we identified the chondroitin 4-sulfotransferase 1 (*C4st1*; *Chst11* – Mouse Genome Informatics) gene as a target of TGFβ and BMP signaling (Klüppel et al., 2002). The *C4st1* gene encodes a Golgi enzyme that catalyzes the transfer of sulfate groups to the 4-O position of chondroitin and dermatan sulfate (Hiraoka et al., 2000; Okuda et al., 2000; Yamauchi et al., 2000). Here, we report on the consequences of inactivation of *C4st1* on cartilage development by using the *C4st1* gene trap ES cell line (*C4st1*^{gt}) to generate mice deficient in *C4st1*. Homozygous mutant mice die within hours of birth and display a severe chondrodysplasia that is restricted to bones formed through endochondral ossification. Detailed analysis of the developing skeleton and the cartilage growth plate showed that loss of *C4st1* disturbs the balance of chondroitin sulfation, causes abnormal chondroitin sulfate localization and leads to strong upregulation of TGFβ signaling with concomitant downregulation of BMP signaling. These defects result in abnormal chondrocyte differentiation and orientation within the growth plate that cause severe disturbances in growth plate morphogenesis.

Materials and methods

Generation of *C4st1* mutant mice

ES cells bearing a gene trap mutation in the *C4st1* gene (*C4st1*^{gt}) were used to generate diploid aggregation chimeras as previously described (Nagy and Rossant, 1993). Offspring transmitting the *C4st1*^{gt} allele through the germline were used to generate homozygous *C4st1*^{gt} animals. Animals were genotyped by Southern analysis was performed according to the manufacturer's recommendations (ZetaProbe, BioRad). DNA from tail biopsies were digested with *PstI* and blotted onto membranes. The membranes were hybridized to a 4.8 kb *en2-lacZ* probe fragment containing *en2*-intronic sequences as well as the *lacZ*-coding sequence. The probe fragment was derived from the PT-1 gene trap vector by *EcoRI-PstI* digestion and was ^{32}P-labeled using an oligo-labeling kit (Pharmacia).

Embryo processing, histology and staining

For Hematoxylin and Eosin, and Safranin O staining, embryos were dissected in PBS and fixed in formalin for several days. Subsequently, embryos were embedded in paraffin, sectioned and stained as previously described. For RNA in situ hybridization and immunofluorescence, embryos were dissected in PBS and fixed in cold 4% PFA/PBS overnight. Tissues were rinsed in cold PBS and cryo-protected by shaking the tissues in cold 0.5 M sucrose/PBS for 12-24 hours. Tissues were embedded in OCT compound (TissueTek), snap-frozen in a dry-ice/ethanol bath and subsequently stored at –70°C. Bones and cartilage of E19.5 mouse embryos were stained with Alizarin Red/Alcian Blue as previously described (McLeod, 1980).

Fluorophore-assisted carbohydrate electrophoresis (FACE)

FACE analysis was performed as previously described (Calabro et al., 2001). Briefly, E18.5 growth plates were separated from the mineralized parts of the bone. Glycosaminoglycans were extracted and enzymatically cleaved to create disaccharides, which were then fluorotagged by reductive amination with 2-aminoacridone. The tagged products are then displayed by electrophoresis, identified by their characteristic migration and chemistry, and quantitated by their molar fluorescence.

RNA in situ hybridization

RNA in situ hybridization on whole-mount E10.0 embryos was performed as previously described (Kluppel et al., 2002). Section RNA in situ hybridization was essentially performed as previously described (Klüppel et al., 1997). Some experiments employed the TSA-Plus DNP (AP) signal amplification kit (Perkin Elmer Life Sciences, Boston).

Immunofluorescence and antibodies

Embryo cryostat sections (7 μm) were air-dried for 2 hours, post-fixed for 10 minutes in 4% paraformaldehyde at room temperature and washed three times with PBS. For the mouse monoclonal 1C6 α-aggrecan antibody [developed by Dr Bruce Caterson and obtained from the Developmental Studies Hybridoma Bank at University of Iowa (DSHB) under the auspices of the NICHD], sections were then digested with 0.1 U of Chondroitinase ABC (Seikagaku, Japan) for 45 minutes at 37°C, followed by three washes with PBS. For the

mouse monoclonal CIIC1 α-collagen II antibody (developed by Drs Rikard Holmdahl/Kristofer Rubin, obtained from DSHB), sections were pre-treated with 2.5% hyaluronidase/PBS for 45 minutes at room temperature, followed by three washes in PBS. Subsequently, sections were blocked, incubated with primary and secondary antibodies and mounted. Primary antibodies and dilutions used were: mouse α-aggrecan 1C6 (DSHB, 1:100), mouse α-collagen II 8A4 (DSHB, 1:100), mouse α-chondroitin-6-sulfate (Seikagaku, 1:100), mouse α-chondroitin-sulfate (Sigma, 1:100), rabbit α-pSmad1 (Cell Signaling, 1:50), rabbit α-pSmad2 (Cell Signaling, 1:50) and rabbit α-Bcl2 (Santa Cruz, 1:200), rabbit α-Bax (Santa Cruz, 1:200). Secondary antibodies were either Cy2 (green) or Cy3 (red) conjugated. For the TUNEL stain, an in situ Cell Death Detection Kit (Roche) was used according to the manufacturer's instructions. For BrdU labeling, pregnant mice were injected twice with 600 μl of 10 mM BrdU (Roche), 5 hours and 2 hours before sacrificing. After sectioning, pictures were taken on a Leica DMR fluorescence microscope and processed with Metamorph software.

Metatarsal explant cultures

The three medial metatarsal bones were removed from the hindlimbs of E18.5 embryos and incubated overnight in explant medium as previously described (Serra et al., 1999). After 24 hours, explants were incubated in medium containing growth factors N-Shh (R&D Systems, 2 μg/ml final concentration), TGFβ (R&D Systems, 500 pM final concentration) or BMP2 (Genetics Institute, 10 nM final concentration) for 4 days, with daily change of medium and growth factors. Subsequently, explants were fixed and processed as described for embryos above.

Results

Severe skeletal abnormalities in mice homozygous for the C4st1^{gt} mutation

The *C4st1* gene trap allele represents an integration of the gene trap vector into the first intron of the *C4st1* gene, thus leading to a fusion transcript containing the first exon of the *C4st1* gene followed by the *lacZ*-coding sequence (Fig. 1A). Mice heterozygous for the *C4st1^{gt}* mutation were fertile and viable.

Table 1. Genotypes of offspring from heterozygous intercrosses at different embryonic and postnatal stages

Age	+/+	+/gt	gt/gt
E9.5-14.5	18 (20.5%)	47 (53.4%)	23 (26.1%)
E18.5	25 (19.5%)	62 (48.5%)	41 (32%)
P21	26 (37%)	44 (63%)	0 (0%)

Offspring of heterozygous matings were genotyped by measuring the ratio of *lacZ* to *en2* DNA (Fig. 1B). In order to determine if this gene trap disrupts *C4st1* function, we analyzed *C4st1* expression in E10.0 wild-type and homozygous mutant embryos using exon-specific probes and RNA whole-mount in situ hybridization (Fig. 1C-F). Although exon I-specific probes visualized the previously reported expression of *C4st1* in the branchial arches and the AER of the developing limb in both wild-type (Fig. 1C) and *C4st1$^{gt/gt}$* (Fig. 1E) embryos, expression of exons II/III was only apparent in wild-type (Fig. 1D), but not *C4st1$^{g/gtt}$* embryos (Fig. 1F). Gene trap integration in the *C4st1* gene thus disrupted expression of exons II and III of the *C4st1* gene, which encode the transmembrane and the intra-Golgi catalytic domains (Fig. 1A); therefore, *C4st1^{gt}* probably represents a null allele of the *C4st1* gene.

Genotypes approximately followed Mendelian ratios up to late embryonic stages (Table 1); however, *C4st1$^{g/gt}$* homozygous mutant animals were not detected 3 weeks after birth (Table 1). Moreover, the Mendelian ratios indicated that the heterozygous state of the *C4st1* gene trap mutation did not result in lethality (Table 1). Homozygous *C4st1$^{g/gt}$* mutant animals were born at normal ratios, but when compared with wild-type animals, displayed severe dwarfism (Fig. 2A) and died within 6 hours of birth with severe respiratory distress (data not shown).

In order to analyze the apparent dwarfism in more detail, we stained the skeleton of E19.5 embryos using Alcian Blue/Alizarin Red (Fig. 2B-H). We observed multiple skeletal

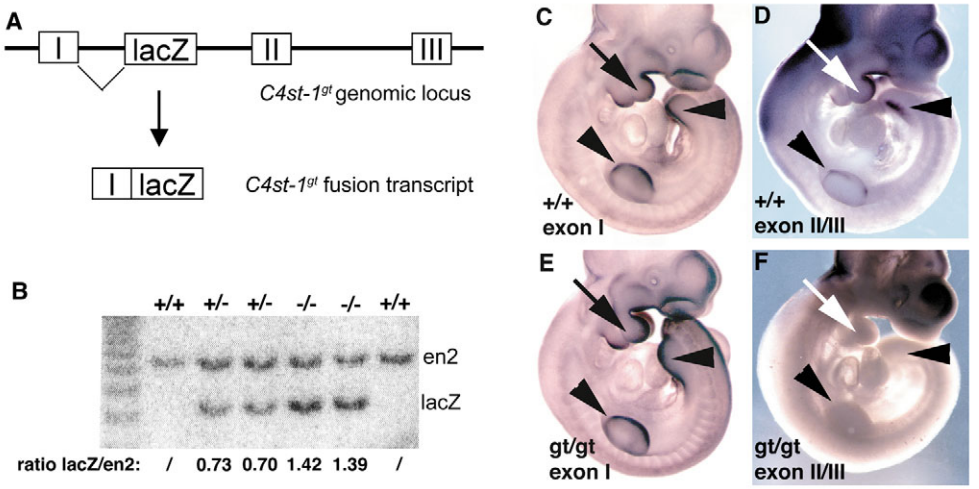

Fig. 1. Gene trap integration into the *C4st1* locus. (A) Schematic representation of the integration of the PT-1 gene trap vector into intron 1 of the mouse *C4st1* locus and the formation of a *C4st1-exonI-lacZ* fusion transcript. (B) Embryos from intercrosses of *C4st1^{gt}* heterozygous animals were genotyped by Southern analysis and the ratio of *lacZ* to en-2 alleles measured. (C-F) Whole-mount in situ hybridization on E10.0 embryos using the indicated exon-specific *C4st1* probes. In branchial arches (white arrows) and AER of limb buds (black arrowheads) in *C4st1* mutant (gt/gt) embryos, a *C4st1* exon I-specific signal (E) is present, but an exon II/III-specific signal (F) is absent.

abnormalities, including a small rib cage, a kinked vertebral column, severely shortened limbs and a dome-shaped skull in mutant embryos (Fig. 2B, part ii). Cartilage staining by Alcian Blue was reduced in homozygote mutant embryos (Fig. 2C, part ii), when compared with wild-type embryos (Fig. 2C, part). Alcian Blue is known to bind GAGs (Hronowski and Anastassiades, 1988; Ippolito et al., 1983), and it has also been reported that undersulfation of proteoglycans leads to reduced Alcian Blue staining (Rossi et al., 1996); thus, the reduction in Alcian Blue staining probably reflects a reduction in GAG content and C4S levels in the cartilage growth plate. Closer inspection of mutant skeletons revealed reduced bone length, but increased width in long bones as well as the iliac bone (Fig. 2C, parts I and ii), and whereas wild-type embryos had well-developed vertebrae with prominent dorsal arches (Fig. 2D, part i), the vertebrae of mutant embryos were misshapen with poorly formed dorsal arches (Fig. 2D, part ii). The length of the mutant scapula was also greatly reduced (Fig. 2E, part ii). We also noted that ossification of the talus (Fig. 2F, part ii) and phalanges two and three was absent in both the fore- and hindlimbs of mutants (Fig. 2F; data not shown), whereas ossification of the calcaneus, the first phalanges and metatarsal bones occurred (Fig. 2F). Finally, we examined skeletal development in mutant heads and found severely shortened facial bones that included the maxilla, mandible and nasal bones (Fig. 2G, part ii), but normal cranial bones (Fig. 2G,H).

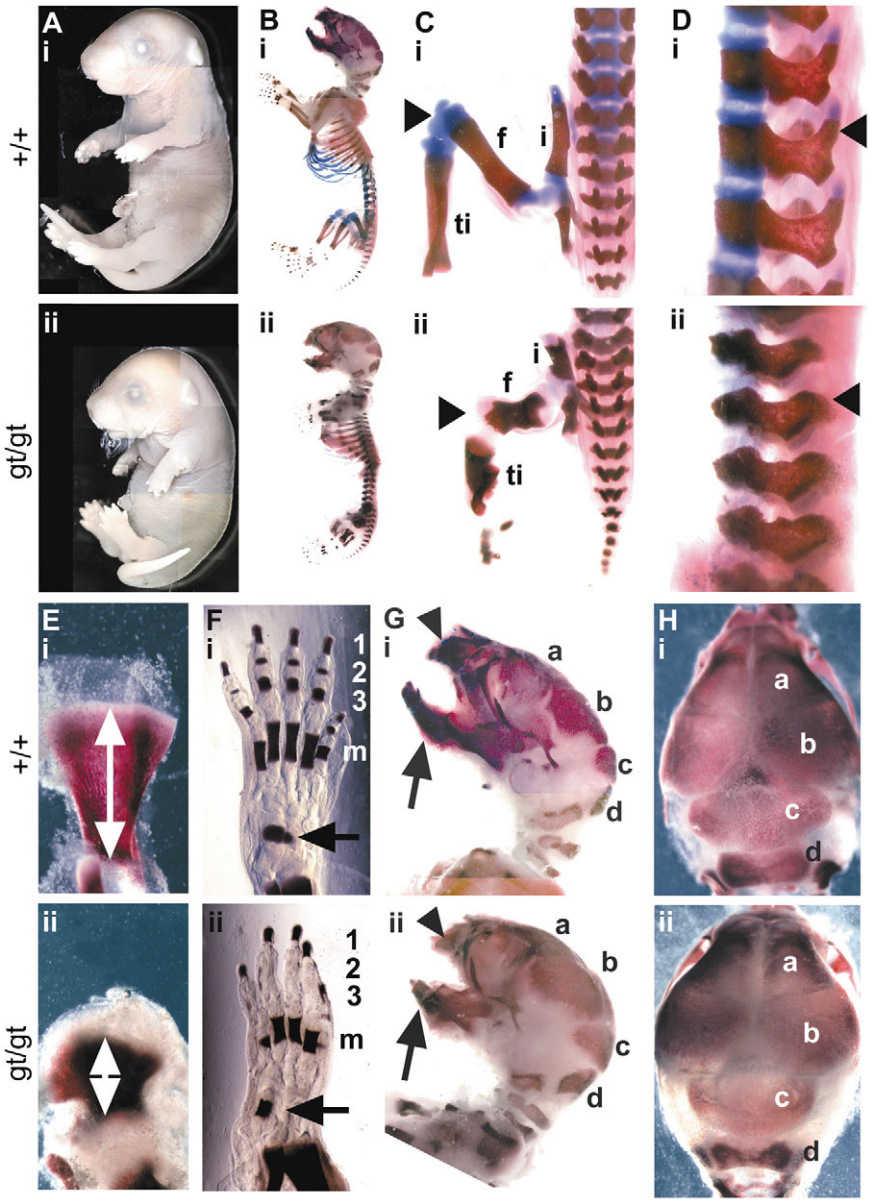

Fig. 2. Phenotype of the *C4st1*^{gt} mutation at E19.5 of embryogenesis. (A) Gross morphology of wild-type (part i, +/+) and *C4st1*$^{gt/gt}$ embryos (ii, part gt/gt). (B-H) Alcian blue/Alizarin Red skeletal stains. (B) Multiple skeletal abnormalities are evident in mutant embryos. (C) Higher magnification of hind limbs, showing the severely shortened and thickened iliac bone (i), femur (f) and tibia and fibula (ti). Arrowhead indicates Alcian Blue staining of cartilage. (D) Vertebrae in the mutant display misshapen dorsal arches (arrowhead). (E) Reduced size of scapula (double-headed while arrow) in mutant embryos. (F) Phalanges 2 and 3, and the talus bone (arrow) fail to ossify in mutant hindlimbs (m, metatarsal bones). (G) Lateral view and (H) dorsal view of skull, showing normal size of frontal (a), parietal (b), interparietal (c) and supraoccipital (d) bones in mutant embryos, but smaller maxilla (arrowhead), mandible (arrow) and nasal bones in mutant embryos.

Altogether, these results demonstrate that *C4st1* is required for morphogenesis of bones formed by endochondral ossification, which includes the long bones of the limb, vertebrae and facial bones; however, it is not required for development of cranial bones, which form through intramembraneous ossification.

The C4st1$^{gt/gt}$ mutation does not affect early cartilage development

Endochondral ossification is a multi-step process that initiates with the aggregation of mesenchymal cells, the subsequent differentiation of these cells into chondrocytes and lastly the coordinated proliferation and differentiation of chondrocytes to form a scaffold for developing bones (Karsenti and Wagner, 2002). We have shown previously that embryos heterozygous for the gene trap mutation in the *C4st1* gene display prominent *lacZ* staining in the developing embryonic cartilage (Klüppel et al., 2002).

To determine which steps of endochondral ossification are affected in *C4st1*$^{gt/gt}$ embryos, we compared the *lacZ* expression pattern in embryos heterozygous and homozygous for this gene trap mutation by both whole-mount staining and sectioning (Fig. 3). At E11.5, we observed identical *lacZ* staining pattern in early cartilage aggregations in the forelimbs of both heterozygous (Fig. 3A, part I; Fig. 3D, part i) and homozygous embryos (Fig. 3A, part ii; Fig. 3D, part ii). At E13.5, staining of cartilage primordia of digits, tibia, fibula

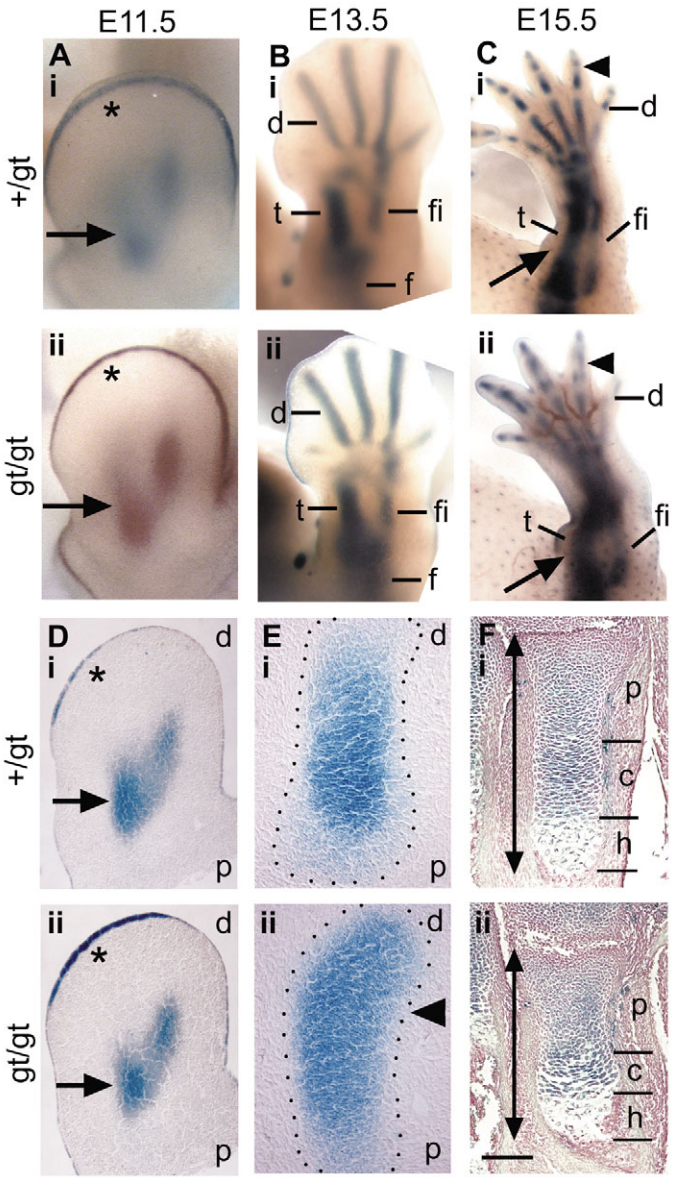

Fig. 3. Analysis of cartilage development in *C4st1*$^{gt/gt}$ embryos by staining for *lacZ*. Part i, wild type; part ii, mutant. (A,D) Identical staining in whole-mount (A) and sectioned (D) forelimb buds of cartilage aggregations (arrows) in +/gt (i) and gt/gt (ii) E11.5 embryos. Asterisk indicates AER. (B,E) Whole-mount staining of cartilage primordia (B) and sectioning of stained tibia primordium (E) at E13.5 in +/gt (i) and gt/gt (ii) hindlimbs shows no differences in size of cartilage elements or cellular patterning. Abbreviations in B: d, digits; t, tibia; fi, fibula; f, femur. Abbreviations in E: d, distal; p, proximal. Arrowhead indicates slight bending of gt/gt tibia primordium. (C) Whole-mount staining of hindlimbs at E15.5, showing impaired segmentation of cartilage in digits (arrowhead) and bending of tibia (arrow) in gt/gt (ii), but not +/gt (i) embryos. d, digits; t, tibia; fi, fibula. (F) Sectioned proximal tibia of stained +/gt (i) and gt/gt (ii) E15.5 hindlimbs. Homozygous mutant growth plates are slightly shortened (double-headed arrow) and show a decrease in the size of the columnar zone (c). p, proliferative zone; h, hypertrophic zone. Scale bar: 100 μm for A,D; 300 μm for B; 100 μm for E; 600 μm for C; 200 μm for F.

and femur were also identical in whole mount preparations of both heterozygous (Fig. 3B, part i) and homozygous embryos (Fig. 3B, part ii), and sectioning of stained limbs revealed no difference in size or cellular structure of these elements (Fig. 3E), although we did note a slight bending of the tibial primordium in homozygous embryos (Fig. 3E, part ii). At E15.5, the overall length of limbs was similar in heterozygous and homozygous embryos (Fig. 3C). By whole-mount *lacZ* staining, limbs from heterozygous embryos revealed staining in all cartilage elements, and a reduction of staining in developing joints and hypertrophic areas (Fig. 3C, part i). Limbs from E15.5 homozygous embryos, however, displayed an impaired segmentation of cartilage in digits that corresponds to the defects in phalange formation we observed at E19.5 and bending of the tibial cartilage was still apparent (Fig. 3C, part ii). Notably, sectioning of the cartilage elements revealed a slightly shortened cartilage growth plate in homozygous embryos (Fig. 3F, part ii), that was accompanied by a reduction in the size of the columnar, but not proliferative or hypertrophic regions (compare Fig. 3F, parts ii and i). Together, these results suggest that mesenchymal aggregation and cartilage primordium formation are not affected in homozygous *C4st1*$^{gt/gt}$ embryos. However, the *C4st1*$^{gt/gt}$ mutation affects chondrocyte differentiation during cartilage growth plate morphogenesis. Furthermore, the severe reduction in bone length observed in E19.5 homozygous embryos was not yet apparent at E15.5, indicating that the effects of the loss of C4st1 on skeletal development readily apparent at E18.5-E19.5 reflect defects in cartilage growth plate function.

The C4st1$^{gt/gt}$ mutation affects growth plate morphogenesis

To investigate the defects in growth plate morphogenesis associated with the loss of C4st1 in more detail, we focused on E18.5 embryos, at which point both skeletal abnormalities and growth plate defects were readily apparent. First, we examined *C4st1* mRNA expression in growth plates by RNA in situ hybridization using the exon 2 and 3 probe (Fig. 4A). *C4st1* was expressed in the proliferating zone of the wild-type growth plate (Fig. 4A, part i), whereas in homozygous mutants, expression of exons 2 and 3 was not observed (Fig. 4A, part ii), consistent with a disruption of *C4st1* expression by the gene trap integration. Next, we examined the growth plate of E18.5 tibias using Safranin O, which stains GAGs in cartilaginous tissue. In mutants, Safranin O staining was reduced, suggesting reduced GAG content (Fig. 4B, part ii) and staining of cartilage islands in wild-type primary bone was absent in the mutants (Fig. 4C). In wild-type growth plates, three distinct chondrocyte subpopulations, namely articular proliferating chondrocytes, columnar proliferating chondrocytes and hypertrophic chondrocytes were readily apparent (Fig. 4B, part i). The morphology of mutant growth plates, however, was disturbed, being severely shortened, disorganized and hypocellular (Fig. 4B, part ii), Consistent with this, the chondrocyte zones and in particular the columnar and hypertrophic zones were reduced in size (Fig. 4B, part ii). To explore the cellular deficits in more detail, we next analyzed Hematoxylin and Eosin-stained growth plates (Fig. 4D-G). This revealed that in the smaller columnar layer of the mutant growth plate, the chondrocyte columns, which

normally form as flattened cells oriented along the longitudinal axis of the developing bone (Fig. 4D, part I; Fig. 4E), were disorganized (Fig. 4D, part ii; Fig. 4F). Strikingly, in the medial region clumps of cells were evident, whereas in the lateral regions, although columns formed, they were not oriented properly and extended radially such that some columns were oriented perpendicular to the long axis of the bone (Fig. 4B, part ii; Fig. 4D, part ii; Fig. 4F, part ii). Interestingly, we also observed an increase in the thickness of the bone collar in *C4st1*$^{gt/gt}$ homozygous mutant growth plates (Fig. 4F). Finally, we examined the Hematoxylin and Eosin stained sections under dark-field conditions, to reveal gross features of the extracellular matrix (ECM). This revealed that wild-type chondrocytes were surrounded by a smooth ECM (Fig. 4G, part i), whereas in the mutants there was extensive fibrillation of the ECM (Fig. 4G, part ii). Of note, this feature is typically found in the cartilage of osteoarthritic patients. Altogether, these results indicate that C4st1 is required for proper chondrocyte development, orientation of chondrocyte stacks and morphogenesis of the cartilage growth plate.

The C4st1$^{gt/gt}$ mutation disturbs chondroitin sulfation balance and chondroitin sulfate spatial distribution in the growth plate

In order to determine how mutation of *C4st1* affected CS sulfation in the growth plate, we quantitated CS species in E18.5 wild-type and mutant embryonic growth plates using fluorophore-assisted carbohydrate electrophoresis (FACE) analysis (Fig. 5A). As expected, chondroitin-4-sulfate (C4S), the product of C4ST, was reduced by more than 90% in homozygous mutant growth plates, suggesting that C4st1 is the main enzyme for production of C4S in cartilage. The presence of a small amount of residual C4S might arise from expression of other C4st1-related enzymes. There was also ~50% drop in chondroitin-6-sulfate (C6S) and a reduction in unsulfated chondroitin (C0S). By contrast, hyaluronan (HA) was only modestly affected in the mutants (Fig. 5A). Therefore, loss of C4st1 effectively reversed the sulfation balance from predominantly C4S in wild type to predominantly C6S in mutant cartilage.

Next, we analyzed the spatial distribution of chondrotin sulfate in E18.5 mutant and wild-type growth

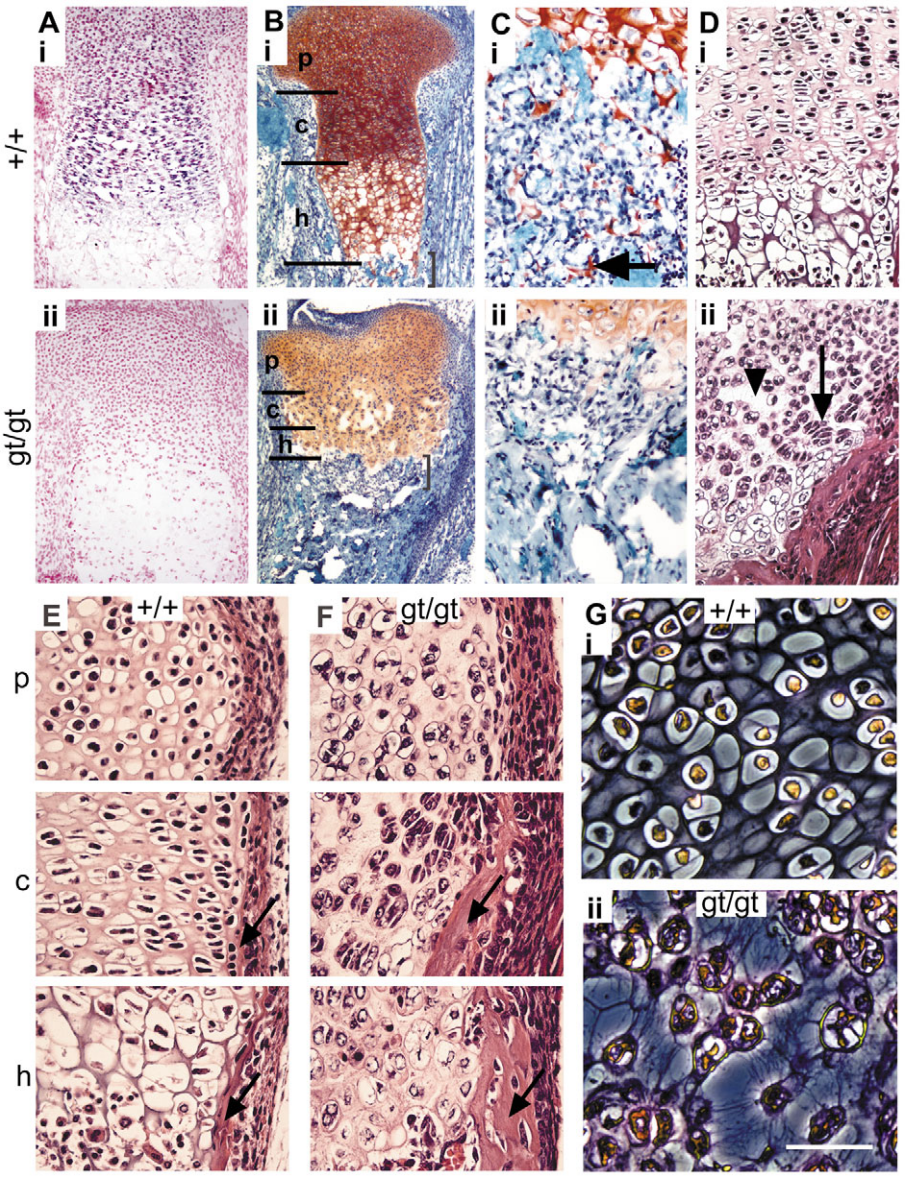

Fig. 4. Cartilage growth plate defects in the proximal tibia of *C4st1*^{gt} mutant embryos at E18.5. (A) RNA in situ hybridization using a *C4st1*-exon2+3-specific probe shows *C4st1* expression in proliferating, but not hypertrophic chondrocytes in wild-type growth plates (i) and the reduction in *C4st1* staining in mutant growth plates (ii). (B,C) Safranin O staining. (B) Safranin O staining shows a reduction in size of proliferating (p), columnar (c) and hypertrophic (h) zones, as well as less intense staining in mutant growth plates (ii) when compared with wild type (i). Brackets indicate areas shown in C. (C) Higher magnification of the transition zone between hypertrophic cartilage and primary bone, showing cartilage islands (arrow) in wild-type (i), but not mutant, bone (ii). (D-G) Hematoxylin and Eosin staining. (D) Mutant growth plates appear disorganized and contain ECM disruptions (arrowhead) and misoriented chondrocyte columns (arrow). (E,F) Higher magnification either wild-type (E) or mutant (F) growth plates (p, c and h are defined in B). Wild-type chondrocyte columns are oriented parallel to the longitudinal bone axis, whereas mutant columns are oriented almost perpendicular to it. In addition there is an increased thickness of the bone collar in the mutants (arrows). (G) Dark-field images of Hematoxylin and Eosin-stained wild-type (i) and mutant (ii) proliferating chondrocytes, showing fibrillation of ECM in mutant growth plates. Scale bar: 400 μm for A; 1 mm for B; 100 μm for C,D; 30 μm for E,F; 10 μm for G.

plates, using antibodies specific to CS and C6S (Fig. 5B-E). αCS antibody, which recognizes chondroitin irrespective of sulfation status, stained the ECM in all three zones of the wild-type growth plate (Fig. 5B), albeit levels in the hypertrophic zone were reduced when compared with other areas. In the periarticular zone of mutant growth plates, CS displayed pericellular and intracellular localization, and was not observed in the ECM (Fig. 5B). However, in the late columnar as well as the hypertrophic zones of homozygous mutant growth plates, CS accumulated in the ECM, and continued to display pericellular and intracellular localization (Fig. 5B). Interestingly, CS staining in the hypertrophic zone again visualized the fibrillation of the mutant ECM. Next, we used an antibody specific to C6S, which revealed that in wild-type growth plates, C6S was restricted to the ECM of the outermost layer of the periarticular zone (Fig. 5C). By contrast, C6S in mutant growth plates was predominantly localized to the pericellular space and extended throughout the periarticular zone and into the columnar layer of the growth plate (Fig. 5C).

To determine if the *C4st1*^{gt} mutation affected the spatial distribution of major cartilage ECM proteins, we analyzed the CS-proteoglycan aggrecan (Fig. 5D) as well as collagen II (Fig. 5E). In all three zones of wild-type growth plates, we observed strong ECM staining for aggrecan (Fig. 5E), whereas in homozygous mutants, aggrecan staining was similar to wild type in the proliferative zone, but displayed a more pericellular deposition in both the columnar and hypertrophic layers (Fig. 5D). Collagen II expression in wild-type growth plates again marked the ECM, with strong labeling in the periarticular and columnar regions and a reduction of staining in the hypertrophic zone (Fig. 5E). Homozygous mutant growth plates showed similar collagen II staining with a typical ECM pattern in all three layers. This indicates that loss of *C4st1*^{gt} does not lead to a general deficiency in ECM. Altogether, these results demonstrate that loss of *C4st1*^{gt} leads to specific defects in chondroitin sulfation balance, a reduction in chondroitin and disturbances in the distribution of chondroitin sulfate.

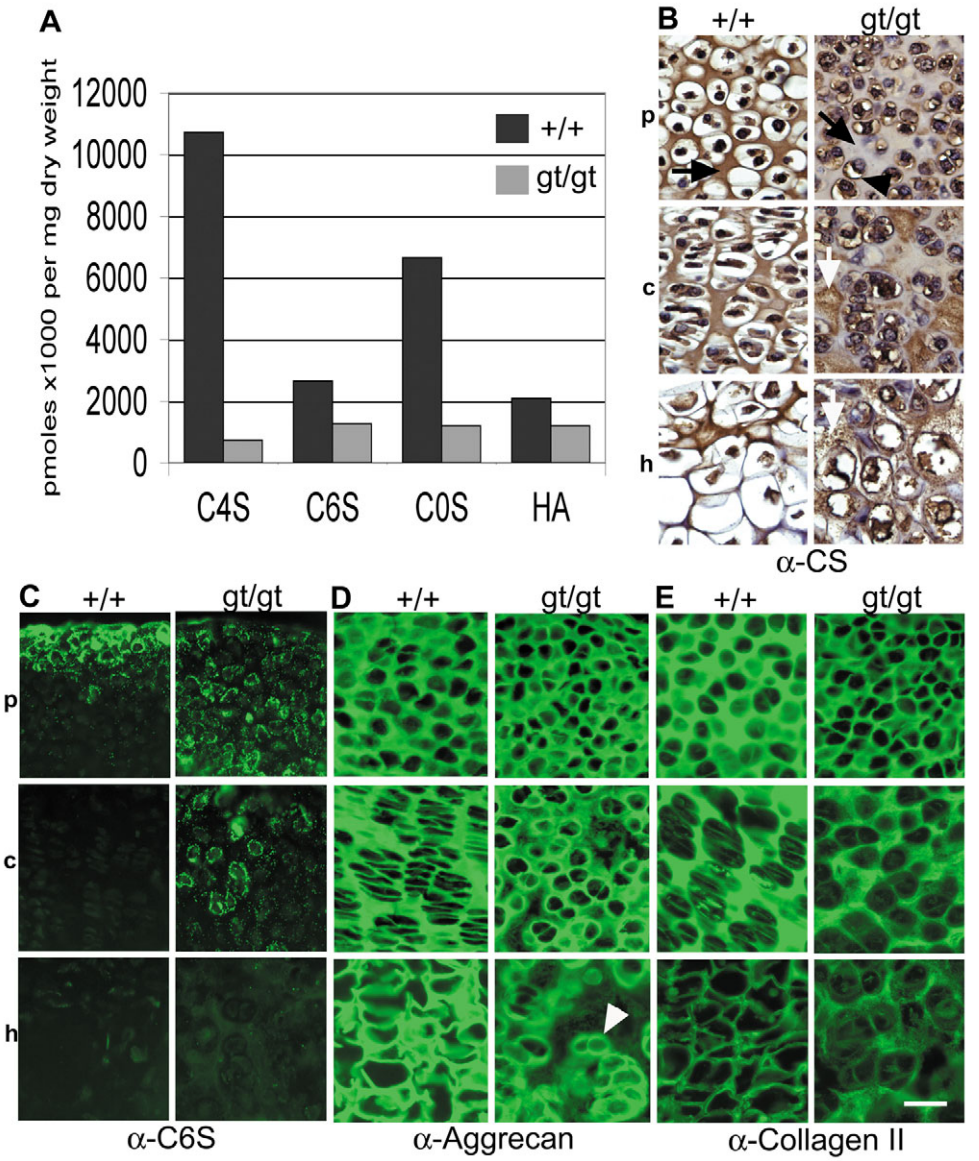

Fig. 5. Analysis of growth plate extracellular matrix (ECM) markers of the proximal tibia at E18.5. (A) Fluorophore-assisted carbohydrate electrophoresis (FACE) analysis of ECM glycosaminoglycans (GAGs). (B) Chondroitin sulfate (CS) immunohistochemistry showing ECM staining (black arrow) in all three growth plate layers (p, proliferating chondrocytes; c, columnar chondrocytes; h, hypertrophic chondrocytes) of wild-type cartilage (+/+), whereas CS staining in mutant (gt/gt) proliferating and columnar layers is restricted to the pericellular space (arrowhead), with very little staining in the ECM (black arrow). However, in the columnar and hypertrophic layers of mutants, ECM staining of CS was observed (white arrows). (C) C6S was detected by immunofluorescence staining and is distributed in the outer-most layers of the proliferative zone in wild-type cartilage (+/+), whereas in mutant cartilage (gt/gt), low pericellular C6S staining was observed in both proliferative and columnar layers. (D) Distribution of aggrecan was analyzed by immunofluorescence, which revealed localization to the ECM in all layers of the wild-type cartilage (+/+), as well as in the proliferative layer of mutant cartilage (gt/gt). However, in the mutant, aggrecan was increasingly restricted to the pericellular space in columnar and hypertrophic (arrowhead) layers. (E) Detection of collagen II by immunofluorescence shows strong staining of the ECM in both wild-type (+/+) and mutant (gt/gt) proliferative and columnar layers, and decreased staining in the ECM of the hypertrophic layer. Scale bar: 10 μm.

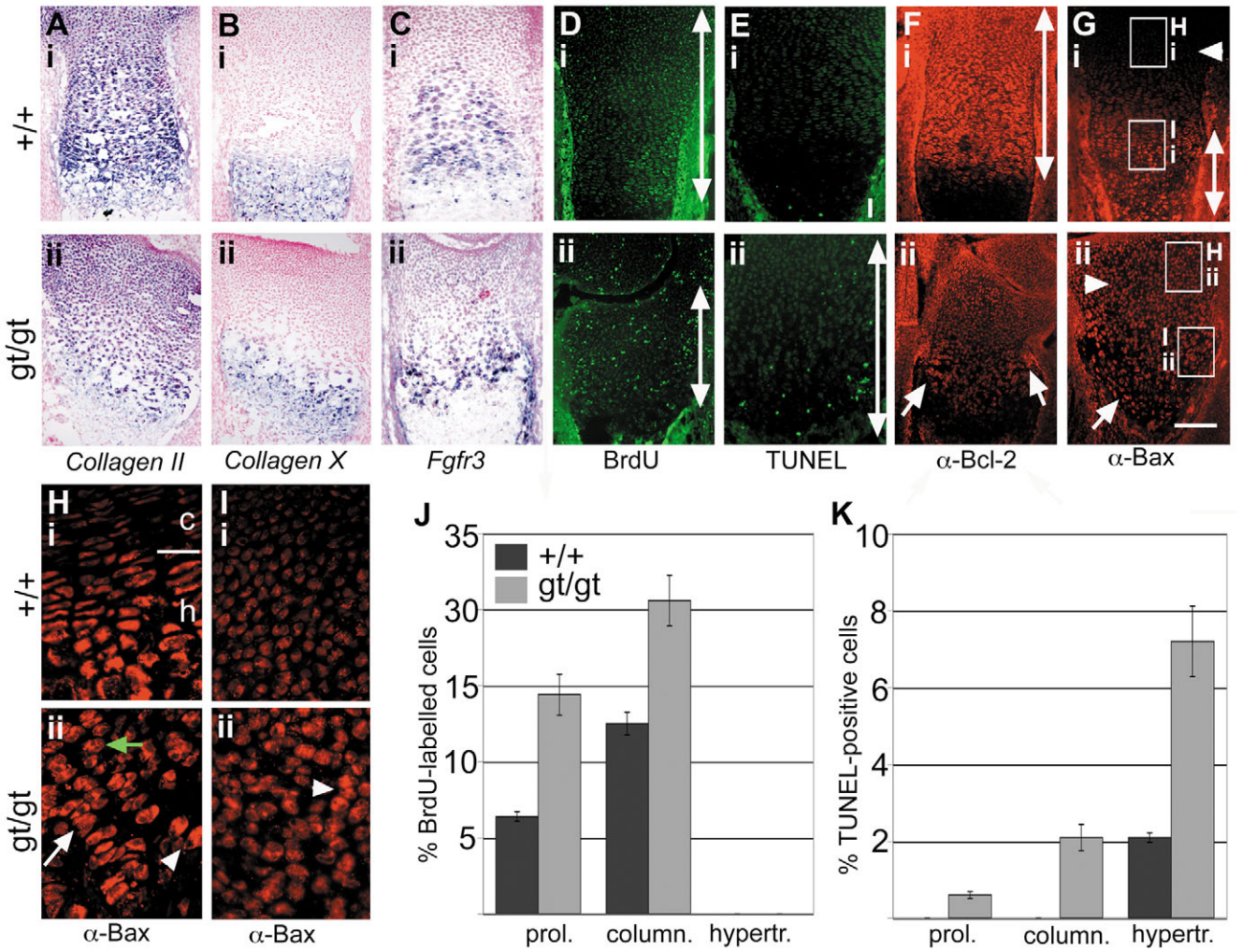

Fig. 6. Chondrocyte development and differentiation at E18.5. (A,B,G-I) Proximal tibia; (C-F) distal tibia. (A-C) Marker analysis by RNA in situ hybridization in wild-type (+/+) and *C4st1*$^{gt/gt}$ (gt/gt) growth plates. Developmental markers for proliferating chondrocytes (collagen II, A), hypertrophic chondrocytes (collagen X, B) as well as columnar chondrocytes (*Fgfr3*, C) were expressed normally in mutant growth plates (ii) when compared with their wild-type counterparts (i), with the size of their expression domains reduced in relation to the overall shortening of the growth plate. (D) BrdU labeling of proliferating chondrocytes was detected by immunofluorescence (green). In wild-type growth plates (i), the zone of proliferation (double-headed arrow) excludes the hypertrophic layer. This proliferative zone is reduced in size in mutant cartilage (ii). (E) TUNEL staining (green) to identify chondrocytes undergoing apoptosis. In wild-type cartilage (i), low numbers of only the most differentiated hypertrophic cells (white bar) showed TUNEL staining, whereas in mutant cartilage, an increased number of cells in all zones (double-headed arrow) showed TUNEL staining (ii). (F) Immunofluorescence (red) using an α-Bcl2 antibody. Wild-type growth plates (i) show widespread Bcl2 staining in the columnar zone (double-headed arrow), whereas staining in gt/gt growth plates (ii) is severely reduced and present only in lateral areas (arrows). (G) Immunofluorescence (red) using an α-Bax antibody. Wild-type growth plates (i) show strong staining in prehypertrophic and hypertrophic chondrocytes (double-headed arrow), but not in columnar and proliferating cells (arrowhead). Homozygous mutant growth plates (ii), however, display staining in hypertrophic cells (arrow) and proliferating cells (arrowhead). (H,I) Higher magnification of regions labeled by white squares in G. Bax expression in wild-type growth plates is restricted to prehypertrophic and hypertrophic cells ('h' in H, i), and is not present in columnar cells ('c' in H, i) or proliferating cells (I, i). White line represents the border between columnar and prehypertrophic and hypertrophic zones. Bax expression in mutant growth plates is observed in hypertrophic cells (arrowhead in H, ii), but also in columnar cells (arrow in H, ii) and proliferating cells (green arrow in H, ii; arrowhead in I, ii). (J) Quantitation of BrdU-labeled cells in proliferating (prol.), columnar (column.) and hypertrophic (hypertr.) chondrocytes. Cartilage in mutant (gt/gt) shows an approximate twofold increase in BrdU-labeled cells in both proliferating and columnar chondrocytes compared with wild type. (K) Quantitation of TUNEL-labeled (apoptotic) cells in all three layers of the growth plate. Mutant growth plates showed a 3.5-fold increase in the number of cells undergoing apoptosis in the hypertrophic zone and apoptotic cells in both proliferating and columnar chondrocytes. Scale bar: 150 μm.

C4st1 regulates proliferation and apoptosis, but not the differentiation pattern of chondrocytes

To determine how alteration in chondroitin sulfation affects chondrocyte differentiation, we first analyzed different chondrocyte subpopulations by marker analysis using RNA in situ hybridization (Fig. 6A-C). The expression patterns of both collagen II (Fig. 6A), a marker for the proliferating zones in the growth plate, and collagen X (Fig. 6B), a marker for

hypertrophic chondrocytes, were indistinguishable between wild-type and homozygous mutant growth plates. Furthermore, expression of fibroblast growth factor receptor type 3 (*Fgfr3*, Fig. 6C), a marker for late columnar proliferating/prehypertrophic chondrocytes, was observed in both wild-type and homozygous mutant growth plates (Fig. 6C, part I; Fig. 6C, part ii). These results indicate that the pattern of chondrocyte differentiation was not significantly affected in *C4st1*^{gt} mutants. Therefore, we examined whether defects in *C4st1*^{gt} growth plate morphology might reflect alterations in the balance of proliferation versus apoptosis (Fig. 6D-I). In wild-type growth plates, proliferation, as measured by BrdU-labeled chondrocytes, was visible throughout the proliferative layers (Fig. 6D, part i), similar to mutant growth plates, although the proliferative zone was drastically reduced in size in mutants (Fig. 6D, part ii). Interestingly, quantitation of proliferation rates in the three growth plate zones revealed an approximately twofold increase in the number of proliferating cells in the proliferative and columnar zones of homozygous mutants, when compared with wild-type growth plates (Fig. 6J). When we examined apoptosis by TUNEL staining (Fig. 6E), we found that wild-type growth plates displayed moderate apoptosis that was restricted to differentiated chondrocytes in the hypertrophic zone (Fig. 6E, part i), whereas mutant growth plates exhibited TUNEL-labeled cells in all zones of the growth plate (Fig. 6E, part ii). Quantitation of TUNEL-positive cells in the three growth plate zones revealed an approximate 3.5-fold increase in TUNEL-positive cells in the hypertrophic zone of homozygous mutant growth plates (Fig. 6K). Moreover, a significant number of TUNEL-positive cells were counted in columnar and proliferating zones of homozygous mutant growth plates, but not in wild-type growth plates (Fig. 6K).

We next wanted to analyze whether this increase in apoptosis correlated with changes in the balance of pro- versus anti-apoptotic signals. For this, we analyzed the expression of the anti-apoptotic protein Bcl2 and the pro-apoptotic protein Bax by immunofluorescence. While wild-type growth plates exhibited a wide expression domain of Bcl2 in proliferating and columnar chondrocytes (Fig. 6F, part i), Bcl2 expression in homozygous mutant growth plates was severely reduced and only present in lateral regions (Fig. 6F, part ii). Conversely, in wild-type growth plates, high levels of Bax expression were observed in prehypertrophic and hypertrophic chondrocytes, but not proliferating or columnar chondrocytes (Fig. 6G, part i; 6H, part i; 6I, part i). Homozygous mutant growth plates also exhibited Bax expression in hypertrophic cells (Fig. 6G, part ii; 6H, part ii), but in contrast to wild-type growth plates, Bax expression was observed in the proliferating zone as well, thus leading to Bax expression in most cells of the mutant growth plates (Fig. 6G, part ii; Fig. 6H, part ii; Fig. 6I, part ii). These results suggest that chondrocytes in mutant cartilage are exposed to imbalanced apoptotic signaling, with a strong reduction in anti-apoptotic signals and an increase in pro-apoptotic signals. Based on these data, we propose that the disturbed morphology of the growth plate reflects both accelerated maturation of chondrocytes leading to severe shortening of the proliferative and hypertrophic zones, as well as enhanced apoptosis of chondrocytes, caused by a disturbed balance of pro- versus anti-apoptotic signals throughout the growth plate region that cannot be compensated by the increased proliferative rate.

The C4st1^{gt} mutation exhibits differential effects on growth factor signaling in the embryonic growth plate

Signaling pathways such as Ihh, BMP and TGFβ and have been shown to be involved in the regulation of chondrocyte development (Karsenty and Wagner, 2002; Minina et al., 2002; Vortkamp, 2001). Therefore, we wanted to determine if the deficiency in chondroitin sulfonation in *C4st1*$^{gt/gt}$ growth plates affected these signaling pathways. For this, we first assessed the expression of target genes or the activity of signaling mediators of these pathways in E18.5 growth plates.

Ihh signaling upregulates expression of *Ptch1*, a negative regulator of hedgehog signaling (Vortkamp, 2001). RNA in situ hybridization showed expression of *Ptch1* in columnar proliferating chondrocytes in both wild-type and mutant growth plates in a similar pattern (Fig. 7A, part i; Fig. 7A, part ii), although the size of the expression domain in mutants was reduced compared with the overall size of the growth plate.

BMP and TGFβ signaling have been shown to lead to the phosphorylation and nuclear translocation of Smad1 and Smad2, respectively, which subsequently control transcriptional responses (Attisano and Wrana, 2002; Massague, 2000; Miyazono et al., 2004; ten Dijke and Hill, 2004). Therefore, to examine BMP signal transduction, we first examined nuclear pSmad1 using a phosphospecific Smad1 antibody. In both wild-type and homozygous mutant growth plates, we observed low background levels of staining in the periarticular and columnar layers (Fig. 7B, part i; Fig. 7B, part ii; Fig. 7C, part I; Fig. 7C, part ii), but prominent nuclear pSmad1 staining was observed in wild-type prehypertrophic and hypertrophic chondrocytes (Fig. 7B, part i; Fig. 7D, part i). However, in the hypertrophic zone of homozygous mutant growth plates, pSmad1 was strongly reduced, with only an occasional cell in the hypertrophic zone displaying nuclear p-Smad1 (Fig. 7B, part ii; Fig. 7D, part ii). When we examined pSmad2, we observed low background levels of staining throughout wild-type growth plates (Fig. 7E, part i; Fig. 7F, part i; Fig. 7G, part i; Fig. 7H, part i), although in the most lateral regions of the proliferative zone and in some hypertrophic cells, we could detect some p-Smad2 (Fig. 7E, part i). In stark contrast, when we examined *C4st1*$^{gt/gt}$ mutant growth plates, we observed a dramatic upregulation of pSmad2 levels (Fig. 7E, part ii), with virtually all cells exhibiting strong nuclear pSmad2 staining (Fig. 7F, part ii; Fig. 7G, part ii; Fig. 7H, part ii). These data demonstrate that whereas the *C4st1*^{gt} mutation has minimal effects on Ihh signaling, it dramatically affects the balance of TGFβ family signaling by strongly downregulating BMP signaling, while potently upregulating TGFβ signaling.

Metatarsal explant cultures: C4st1$^{gt/gt}$ growth plates retain the capacity to respond to exogenous growth factors

To determine whether growth plates in *C4st1*^{gt} mutant animals have an inherent alteration in their ability to respond to distinct extracellular cues, we analyzed the potential of wild-type and mutant metatarsal bone explants to respond to exogenously added growth factors. Metatarsal bones from E18.5 wild-type

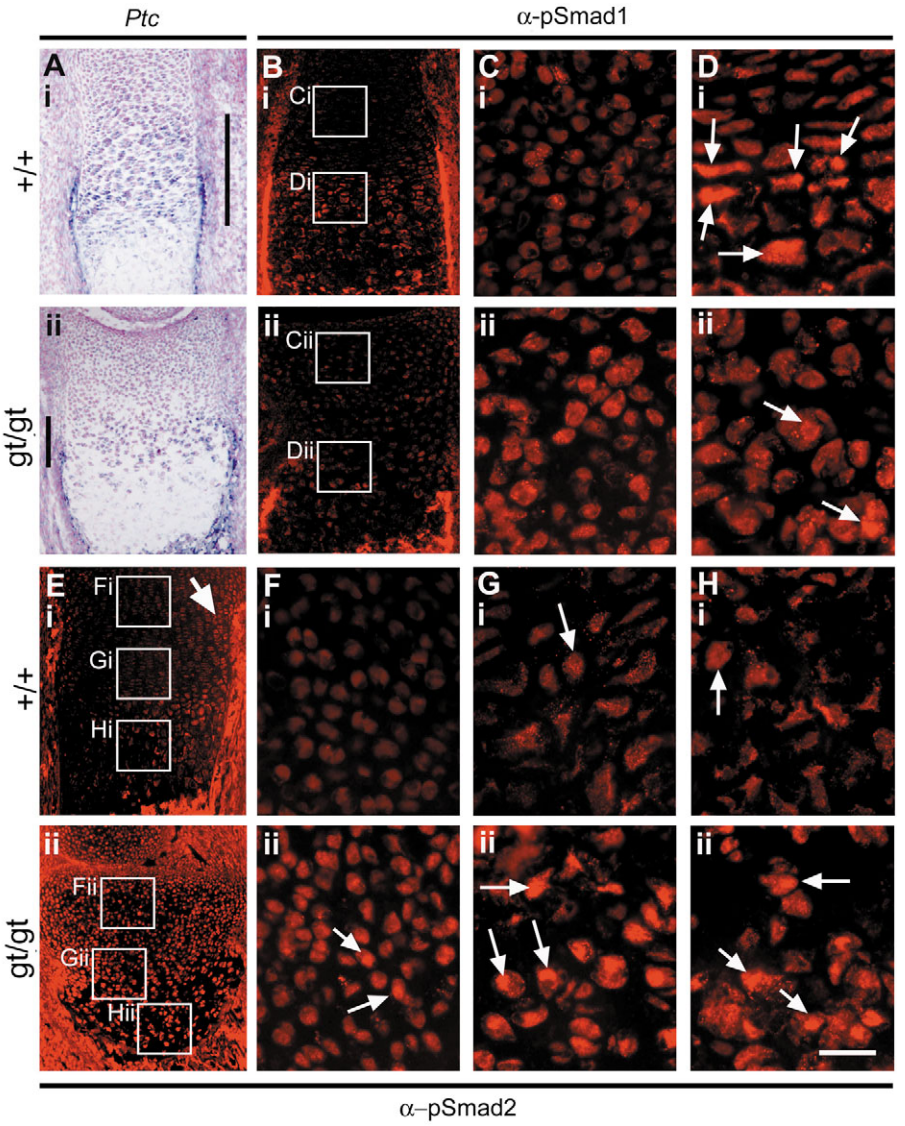

Fig. 7. Analysis of Ihh, BMP and TGFβ signaling in E18.5 cartilage. (A) distal tibia; (B-H) proximal tibia. (A) *Ptch1* RNA in situ hybridization as output for Ihh signaling reveals expression in columnar chondrocytes in both wild-type (i) and mutant (ii) cartilage. (B-D) Phosphorylated Smad1 distribution. Wild-type (i) and mutant (ii) growth plates were stained using an antibody that recognizes Smad1 phosphorylated by activated BMP receptors. (B) pSmad1 (red) is seen in hypertrophic chondrocytes in wild-type cartilage (i), and is reduced in mutant cartilage (ii). (C) Higher magnification of proliferating region (indicated as 'C' in B) shows very little pSmad1 staining in both wild-type (i) and mutant (ii) cartilage. (D) Higher magnification of early hypertrophic regions (indicated as 'D' in B) shows nuclear pSmad1 staining in wild-type chondrocytes (i), which is reduced in mutant chondrocytes (ii). (E-H) Phosphorylated Smad2 distribution. Wild-type and mutant growth plates were stained using an antibody that recognizes Smad2 phosphorylated by activated TGFβ receptors. (E) Very little nuclear pSmad2 staining was seen in wild-type growth plates (i) in columnar/early hypertrophic layers and in lateral aspects of the growth plate (white arrow). In mutant cartilage (ii), strong pSmad2 staining is seen in all cartilage layers. (F-H) Higher magnification of regions indicated in E. Arrows indicate nuclear staining. (F) Higher magnification of proliferative layer. No nuclear pSmad2 staining was seen in wild-type chondrocytes (i), whereas a high proportion of mutant chondrocytes (ii) shows moderate nuclear pSmad2 staining. (G) Higher magnification of late columnar layer. Very little nuclear pSmad2 staining is visible in wild-type cells (i), whereas strong nuclear pSmad2 staining is apparent in all mutant chondrocytes (ii). (H) Higher magnification of hypertrophic layers. Weak nuclear pSmad2 staining is seen in few wild-type chondrocytes (i), whereas almost all mutant chondrocytes show strong nuclear pSmad2 staining (ii). Scale bar: 300 μm for A; 200 μm for B,E; 20 μm for C,D,F,G,H.

and mutant embryos were dissected and cultured for 4 days in the absence or presence of TGFβ1, BMP2 and N-Shh, which has been shown to mimic the effects of Ihh (Deckelbaum et al., 2002). The explants were then analyzed for gross morphological changes as well as sectioned to examine growth plate hypertrophy, as measured by *Collagen X* mRNA expression and the activity of Ihh, TGFβ and BMP signaling.

Treatment of both wild-type and *C4st1*$^{gt/gt}$ mutant explants with N-Shh decreased the size of the mineralized part of the explants and increased the size of the non-mineralized part (Fig. 8A), albeit to a lesser degree in the mutants (Fig. 8B). In both wild-type and homozygous mutant explants, N-Shh induced *Ptch1* expression (Fig. 8E,F) and strongly suppressed collagen X expression (Fig. 8C,D), consistent with its reported role in blocking hypertrophy. Furthermore, we noted no significant differences in the response of the cartilage component of wild-type versus mutant growth plates in any of these assays. However, we did note in this assay that the perichondrium in *C4st1*$^{gt/gt}$ mutant explants underwent neither N-Shh-induced thickening (arrow Fig. 8C,D), nor N-Shh-induced *Ptch1* expression (Fig. 8E, part ii; Fig. 8F, part ii), contrasting wild-type perichondrium (arrow Fig. 8E, part i; Fig. 8F, part i). Next, we examined exogenous TGFβ stimulation, which led to a decrease in both length and width of metatarsal explants (Fig. 8A,B) and reduction of collagen X expression (Fig. 8C,D). When we examined pSmad2 levels in untreated wild-type metatarsals, some nuclear pSmad2 was evident in prehypertrophic and hypertrophic chondrocytes (Fig. 8G-I; Fig. 8G, part iii; Fig. 8G, part iv), and this was strongly increased by TGFβ in the prehypertrophic and hypertrophic zones, which were also reduced in size (Fig. 8H,I; Fig. 8H, part iii; Fig. 8H, part iv), in agreement with TGFβ-dependent reduction in collagen X expression. In the proliferative zone, there was very little discernible pSmad2

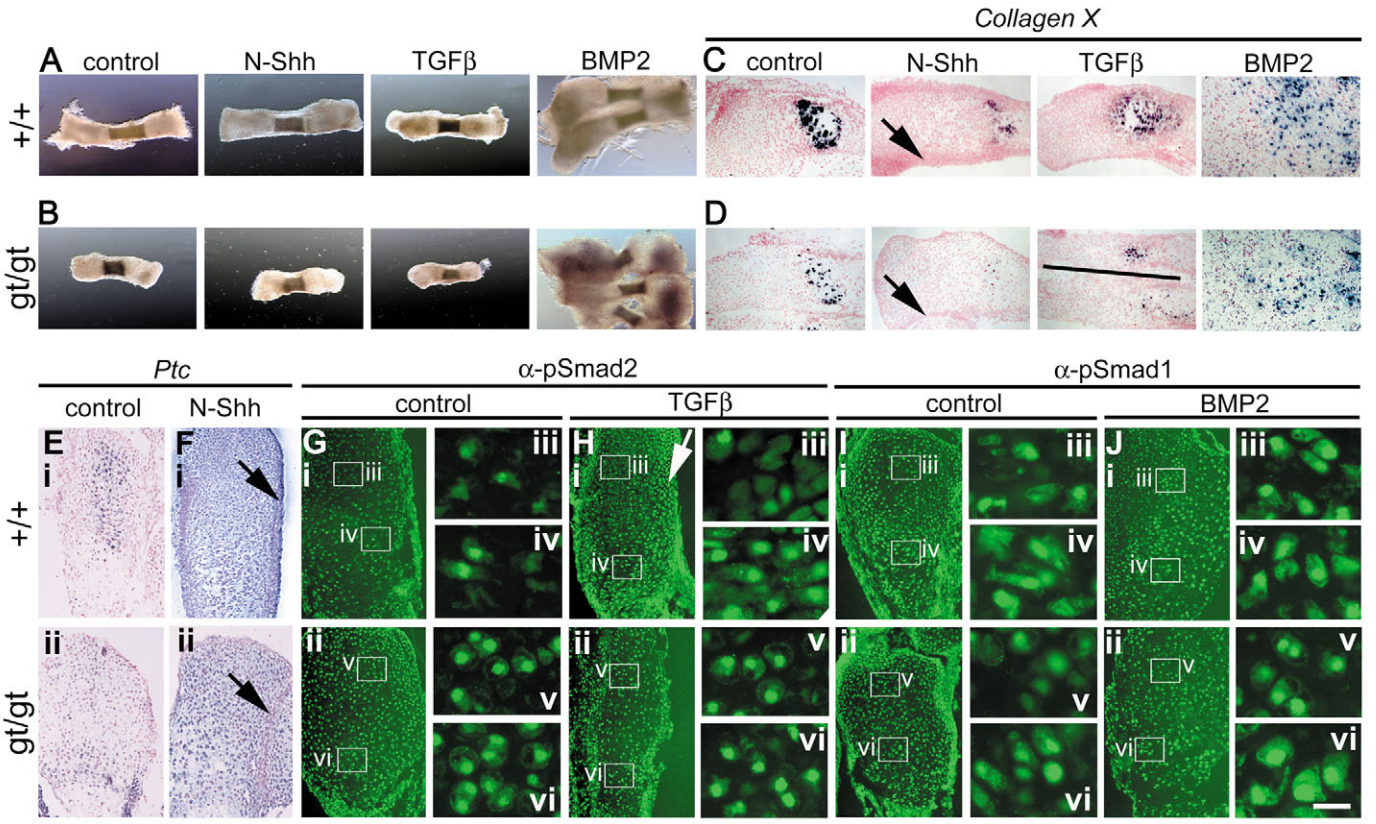

Fig. 8. *C4st1*$^{gt/gt}$ metatarsal explants are able to respond to exogenous growth factors. Metatarsals were removed from E18.5 wild-type (+/+) and mutant (gt/gt) embryos and cultures for 4 days in either the absence (control) or presence of 2 μg/ml N-Shh, 500 pM TGFβ or 10nM BMP2 as indicated. Metatarsals were photographed (A,B) or processed for RNA in situ hybridization (C-F) or immunofluorescence (G-J). (A,B) Appearance of explants after 4 day treatment with no factor (control), N-Shh, BMP2 or TGFβ. (C,D) Effects of growth factor treatment on hypertrophic differentiation as visualized by collagen X RNA in situ hybridization. Collagen X staining is reduced in N-Shh and TGFβ-treated wild-type (C) and mutant (D) explants and increased in BMP2-treated wild-type and mutant explants. In addition, treatment of wild-type, but not mutant explants with N-Shh lead to increased thickness of the perichondrium (arrows). (E-J) Signaling pathways in metatarsal explants. (E) *Ptch1* staining in untreated wild-type and mutant explants is restricted to proliferating chondrocytes. No *Ptch1* expression is seen in the perichondrium. (F) Treatment of explants with N-Shh leads to *Ptch1* expression throughout the growth plate in both wild-type and mutant explants. Wild-type explants also showed *Ptch1* expression in the perichondrium, which was not observed in mutant explants (arrows). (G) Nuclear pSmad2 staining in untreated wild-type explants was seen in some late columnar/early hypertrophic cells (i; see iv for higher magnification), whereas occasional weak staining in proliferating cells was also present (i; iii). In untreated mutant explants, strong pSmad2 staining was apparent in all cells of the growth plate (ii, v, vi). (H) Treatment of wild-type explants with TGFβ lead to an increase in the number of pSmad2-stained cells and staining intensity in hypertrophic cells (i, iv), whereas cells in the proliferative layer were still mostly negative for nuclear pSmad2 (i, iii). Arrow in i indicates increased pSmad2 staining in lateral regions of the growth plate. Treatment of mutant explants with TGFβ lead to a small increase in pSmad2 staining intensity (ii, v, vi). (I) Nuclear pSmad1 expression in untreated wild-type explants was apparent in a subset of proliferating chondrocytes (iii) and in hypertrophic chondrocytes (iv). Whereas mutant explants also showed nuclear pSmad1 staining in hypertrophic chondrocytes (ii, vi), staining intensity was lower in proliferating chondrocytes (ii, v). (J) Both wild-type (i, iii, iv) and mutant (ii, v, vi) explants treated with BMP2 showed strong nuclear pSmad1 staining in the expanded region of hypertrophy (iii, iv, v, vi). Scale bar: 5 mm for A,D; 1 mm for C-F; 500 μm for G-J, parts i, ii; 20 μm for G-J, parts iii-vi.

staining in untreated wild-type growth plates (Fig. 8G, part i; Fig. 8G, part iii), whereas after TGFβ treatment, staining became apparent in the lateral regions (arrow in Fig. 8H, part i), with most cells in the center remaining pSmad2-negative even after TGFβ treatment (Fig. 8H, part iii). These results are in accordance with our in vivo observations on the activity of the Smad2 pathway in wild-type growth plates. The *C4st1*$^{gt/gt}$ explants also recapitulated our in vivo results, displaying strong nuclear pSmad2 staining in virtually all cells of the growth plate, including chondrocytes in the proliferative zone, even in the absence of TGFβ stimulation (Fig. 8G, part ii; Fig. 8G, part v; Fig. 8G, part vi), although addition of TGFβ caused some further enhancement (Fig. 8H, part ii; Fig. 8H, part v; Fig. 8H, part vi). This suggests that the constitutively activated TGFβ signaling pathway in mutant chondrocytes can be further stimulated by exogenous TGFβ.

In sharp contrast to TGFβ, treatment with BMP2 caused a dramatic increase in the size of both wild-type and mutant growth plates (Fig. 8A,B), as well as inducing collagen X expression (Fig. 8C,D). We next examined pSmad1, which was present mainly in prehypertrophic and hypertrophic zones, consistent with our in vivo analyses, although we also observed some pSmad1 in a subset of proliferating chondrocytes (Fig. 8I, part i; Fig. 8I, part iii; Fig. 8I, part iv). Treatment with

Development

BMP2 led to an expansion of the hypertrophic domain of pSmad1 staining (Fig. 8J, part i; Fig. 8J, part iii; Fig. 8J, part iv). By contrast, we observed that pSmad1 was reduced in untreated *C4st1*$^{gt/gt}$ explants (Fig. 8I, part ii) and was restricted to a small region of hypertrophic chondrocytes (Fig. 8I, part ii; Fig. 8I, part v; Fig. 8I, part vi). However, treatment with BMP2 led to a significant induction in pSmad1 (Fig. 8J, part ii; Fig. 8J, part v; Fig. 8J, part vi), corroborating our morphological and gene expression data that *C4st1*$^{gt/gt}$ explants have the capability to respond to BMP signaling.

Altogether, these results demonstrate that while the balance of TGFβ and BMP signaling are disturbed in vivo, mutant growth plates retain the inherent capacity to respond to exogenous growth factors. *C4st1*^{gt} mutant metatarsal explants were able to respond to exogenous BMP2 and also to TGFβ, despite the constitutive activation of this pathway. Thus, interfering with chondroitin-4-sulfation causes spatial pathway-specific defects in the elaboration of morphogen signaling in the cartilage growth plate.

Discussion

We have demonstrated that mice with a mutation in *C4st1* die shortly after birth with severe chondrodysplasia, altered chondrocyte stack orientation and accelerated chondrocyte differentiation. We show that the reduction in C4S in *C4st1*$^{gt/gt}$ mutant mice leads to changes in the spatial distribution of CS and affects the balance of TGFβ family signaling in the cartilage growth plate (Fig. 8). Thus, correct chondroitin sulfation balance is essential for mammalian cartilage morphogenesis and embryonic development.

Cartilage growth plate morphogenesis requires functional C4st1

Disruption of expression of C4st1 did not interfere with early steps in endochondral ossification, including mesenchymal aggregation and cartilage primordia formation. However, cartilage growth plate morphogenesis was disturbed. This was not due to defective growth plate patterning, but to a severe reduction in the size of the proliferating, columnar and hypertrophic zones. Further, cartilage islands that are evident in the region of primary bone in wild-type long bones were absent in the mutants. In addition, we observed a strong increase in the rate of apoptosis in the mutant growth plates, caused by an imbalance of pro- versus anti-apoptotic signals. All of these results are consistent with a model (Fig. 9) in which chondrocytes in mutant growth plates undergo accelerated differentiation and apoptosis that leads to reduced growth plate size and subsequent bone length.

We also demonstrated an altered orientation of mutant chondrocyte stacks, leading to stacks that are oriented perpendicular to the longitudinal axis of the bone. This has not, to the best of our knowledge, been reported previously. This phenotype might be related to physical changes in the growth plate. Alternatively, there is evidence for an as yet unidentified periarticular factor that provides an instructive signal for chondrocyte stack orientation (Abad et al., 2002). It is tempting to speculate that chondroitin sulfation may control the transmission or reception of such a signal thereby controlling the polarity of chondrocyte stacks. Future analysis of *C4st1*$^{gt/gt}$ growth plates will give more insight into this phenotype. The orientation of chondrocyte stacks along the longitudinal axis of the bone is considered a key determinant of bone longitudinal growth and morphogenesis (Karsenty and Wagner, 2002; Shum et al., 2003). Therefore, the altered orientation of stacks in mutant growth plates might be an important contribution to the reduced longitudinal growth of the mutant embryonic long bones and their enhanced thickness.

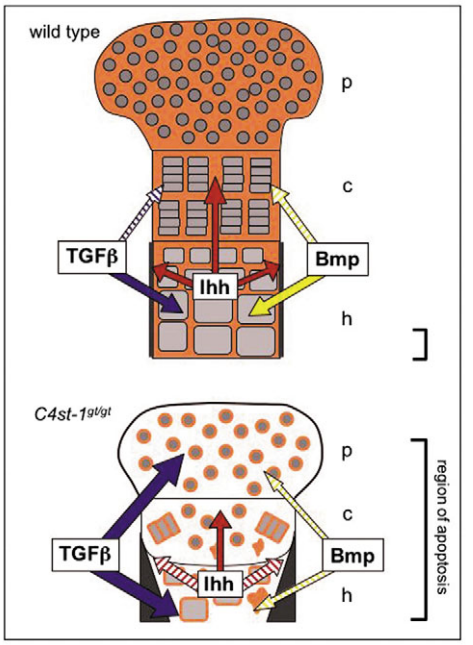

Fig. 9. Model of the role of C4st1 during cartilage development. The organized growth plate of wild-type cartilage contains proliferating (p), columnar (c) and hypertrophic (h) chondrocytes (grey) surrounded by ECM containing CS (orange). *C4st1*$^{gt/gt}$-mutant growth plates are severely reduced in length, but display increased width. The chondrocyte layers are disorganized and chondrocyte columns are not oriented along the longitudinal axis of the bone. CS (orange) is mostly absent from the ECM and instead is located in the pericellular space surrounding chondrocytes. There is a dramatic increase in the thickness of the bone collar (dark grey) in mutant growth plates and bone. Whereas Ihh signaling to proliferating chondrocytes is not significantly altered in mutant growth plates (red arrows), BMP signaling to both proliferating and hypertrophic chondrocytes is reduced (yellow arrows), and TGFβ signaling to proliferating and hypertrophic chondrocytes (blue arrows) is dramatically increased in mutant growth plates. Imbalance in apoptotic signals leads to a dramatic increase in the area prone to undergo apoptosis (indicated by black brackets).

Altered growth factor signaling in C4st1$^{gt/gt}$ growth plates

A prominent defect in the cartilage of *C4st1*$^{gt/gt}$ mutant growth plates is a marked reduction in both the proliferative and hypertrophic zones. A number of signaling pathways have been shown to be involved in controlling cartilage morphogenesis (Karsenty and Wagner, 2002; Vortkamp, 2001). Of particular note, BMP family members positively regulate chondrocyte proliferation and hypertrophy, but negatively regulate terminal chondrocyte differentiation both in vitro and in vivo (Yoon and Lyons, 2004). This results in BMPs increasing the length of the proliferative and hypertrophic zones (Minina et al., 2002).

TGFβ1, conversely, negatively regulates chondrocyte proliferation and hypertrophy (Serra and Chang, 2003). Our analysis of Smad signaling in *C4st1*$^{gt/gt}$ mutant growth plates revealed that active Smad1, which functions in the BMP pathway, was downregulated, whereas Smad2 in the TGFβ pathway was strongly upregulated throughout the growth plate. Therefore, the combination of reduced BMP signaling and upregulation of TGFβ signaling probably plays a key role in causing the severe reduction in the size of the proliferative and hypertrophic zones and increased apoptosis observed in *C4st1*$^{gt/gt}$ mutant growth plates (Fig. 9). These results contrast the relatively normal spatial activation of the hedgehog pathway we observed, suggesting that the lack of C4S does not have a major impact on the function of Ihh during growth plate morphogenesis. These results suggest that the lack of C4S has specific effects on selected growth factor signaling pathways in the growth plate.

It is unclear what molecular mechanism underlies altered TGFβ family signaling in *C4st1*$^{gt/gt}$ mutant growth plates. However, mutant metatarsal explants treated with exogenous BMP2 responded with an increase in explant size, collagen X expression and Smad1 activation. Therefore, the loss of BMP signaling in the mutants is not due to an intrinsic inability of the cells to respond to BMP. Therefore, expression of endogenous BMP ligands may be affected, or the ability of BMPs to diffuse or access all surface signaling receptors may be compromised. Alternatively, TGFβ ligand has been shown to interact with the small leucine-rich CS-containing proteoglycans, Decorin and Biglycan, which modulate TGFβ activity. Of particular relevance, Decorin negatively regulates TGFβ signaling (Hildebrand et al., 1994; Kresse and Schonherr, 2001). As the distribution of CS and the CS-proteoglycan aggrecan were shifted to the pericellular environment of the proliferating and hypertrophic zones in mutant growth plates, altering the balance of CS sulfation may interfere with the proper sequestration of TGFβ in the ECM and allow for constitutive TGFβ signaling. Finally, studies in *Xenopus* and mammalian cell culture models have highlighted dose-dependent antagonistic crosstalk between TGFβ and BMP signaling pathways (Candia et al., 1997). Thus, strong upregulation of TGFβ signaling in the mutants may indirectly antagonize endogenous BMP signals.

The absence of C4st1 leads to osteoarthritis-like symptoms

C4st1$^{gt/gt}$ mutant growth plates are disorganized, hypocellular, display accelerated chondrocyte maturation and have a fibrillated ECM. Furthermore, there is a reduction in GAG content and CS and in particular aggrecan content in mutant growth plates. Many of these cartilage growth plate deficiencies are characteristic of the degenerative changes that occur in the cartilage in osteoarthritis (OA) (Martel-Pelletier, 2004). Treatment with C4S and CS can prevent cartilage degradation, partially by inhibiting the catabolism of proteoglycans and collagens (Uebelhart et al., 1998). Thus, *C4st1*$^{gt/gt}$ mice with their reduction in cartilage C4S and CS levels have features of an osteoarthritic phenotype. TGFβ signaling has been shown to have a dual role during OA: while it can counteract GAG loss, it also promotes the development of osteophytes, the occurrence of which is strongly associated with OA (Scharstuhl et al., 2002). Moreover, BMP signaling has also been implicated in a protective role during OA development (Rountree et al., 2004; Scharstuhl et al., 2003). Thus, the combined reduction in BMP signaling and upregulation in TGFβ signaling might be functionally involved in the development of OA-like symptoms in *C4st1*-mutant mice.

Mutations in the latency-associated peptide (LAP) domain of TGFβ1 leads to secretion of constitutively active TGFβ1 ligand are associated with Camurati-Engelmann disease in humans (Campos-Xavier et al., 2001; Janssens et al., 2000; Janssens et al., 2003; Saito et al., 2001). This condition is characterized by a thickening of the bone collar of the long bones. In *C4st1*$^{gt/gt}$ long bones, we also observed a strong increase in the thickness of the bone collar, suggesting that the observed upregulation of TGFβ signaling may have a similar effect as that observed in individuals with Camurati-Engelmann disease.

Conclusion

In summary, we have shown that the correct balance of chondroitin sulfation is crucial for endochondral bone formation. Disruption of the *C4st1* locus leads to chondrodysplasia, osteoarthritis-like symptoms and affects the balance of TGFβ family signaling in the cartilage growth plate. These results thus demonstrate a crucial role for a chondroitin sulfotransferase in mammalian development and disease.

We thank Ken Harpal for the Hematoxylin and Eosin staining, and the histology laboratory in the Department of Pathology in Mount Sinai Hospital for the Safranin O staining. This work was funded by the Canadian Institutes of Health Research (CIHR) to J.L.W. M.K. was supported by postdoctoral fellowships from CIHR and the Canadian Association of Gastroenterology. J.L.W. is a CIHR Investigator and an International Research Scholar of the Howard Hughes Medical Institute.

References

Abad, V., Meyers, J. L., Weise, M., Gafni, R. I., Barnes, K. M., Nilsson, O., Bacher, J. D. and Baron, J. (2002). The role of the resting zone in growth plate chondrogenesis. *Endocrinology* **143**, 1851-1857.

Attisano, L. and Wrana, J. L. (2002). Signal transduction by the TGF-beta superfamily. *Science* **296**, 1646-1647.

Baur, S. T., Mai, J. J. and Dymecki, S. M. (2000). Combinatorial signaling through BMP receptor IB and GDF5: shaping of the distal mouse limb and the genetics of distal limb diversity. *Development* **127**, 605-619.

Calabro, A., Midura, R., Wang, A., West, L., Plaas, A. and Hascall, V. C. (2001). Fluorophore-assisted carbohydrate electrophoresis (FACE) of glycosaminoglycans. *Osteoarthr. Cartilage* **9**, S16-S22.

Campos-Xavier, B., Saraiva, J. M., Savarirayan, R., Verloes, A., Feingold, J., Faivre, L., Munnich, A., Le Merrer, M. and Cormier-Daire, V. (2001). Phenotypic variability at the TGF-beta1 locus in Camurati-Engelmann disease. *Hum. Genet.* **109**, 653-658.

Candia, A. F., Watabe, T., Hawley, S. H., Onichtchouk, D., Zhang, Y., Derynck, R., Niehrs, C. and Cho, K. W. (1997). Cellular interpretation of multiple TGF-beta signals: intracellular antagonism between activin/BVg1 and BMP-2/4 signaling mediated by Smads. *Development* **124**, 4467-4480.

Deckelbaum, R. A., Chan, G., Miao, D., Goltzman, D. and Karaplis, A. C. (2002). Ihh enhances differentiation of CFK-2 chondrocytic cells and antagonizes PTHrP-mediated activation of PKA. *J. Cell. Sci.* **115**, 3015-3025.

Garcia-Garcia, M. J. and Anderson, K. V. (2003). Essential role of Glycosaminoglycans in Fgf signaling during mouse gastrulation. *Cell* **114**, 727-737.

Grobe, K., Ledin, J., Ringvall, M., Holmborn, K., Forsberg, E., Esko, J. D. and Kjellen, L. (2002). Heparan sulfate and development: differential

roles of the N-acetylglucosamine N-deacetylase/N-sulfotransferase isozymes. *Biochim. Biophys. Acta* **1573**, 209-215.
Habuchi, O. (2000). Diversity and functions of glycosaminoglycan sulfotransferases. *Biochim. Biophys. Acta* **1474**, 115-127.
Hildebrand, A., Romaris, M., Rasmussen, L. M., Heinegard, D., Twardzik, D. R., Border, W. A. and Ruoslahti, E. (1994). Interaction of the small interstitial proteoglycans biglycan, decorin and fibromodulin with transforming growth factor beta. *Biochem. J.* **302**, 527-534.
Hiraoka, N., Nakagawa, H., Ong, E., Akama, T. O., Fukuda, M. N. and Fukuda, M. (2000). Molecular cloning and expression of two distinct human chondroitin 4-O-sulfotransferases that belong to the HNK-1 sulfotransferase gene family. *J. Biol. Chem.* **275**, 20188-20196.
Horiki, M., Imamura, T., Okamoto, M., Hayashi, M., Murai, J., Myoui, A., Ochi, T., Miyazono, K., Yoshikawa, H. and Noriyuki, T. (2004). Smad6/Smurf1 overexpression in cartilage delays chondrocyte hypertrophy and causes dwarfism with osteopenia. *J. Cell Biol.* **165**, 433-445.
Hronowski, L. J. and Anastassiades, T. P. (1988). Detection and quantitation of proteoglycans extracted from cell culture medium and cultured cartilage slices. *Anal. Biochem.* **174**, 501-511.
Ippolito, E., Pedrini, V. A. and Pedrini-Mille, A. (1983). Histochemical properties of cartilage proteoglycans. *J. Histochem. Cytochem.* **31**, 53-61.
Janssens, K., Gershoni-Baruch, R., Guanabens, N., Migone, N., Ralston, S., Bonduelle, M., Lissens, W., Van Maldergem, L., Vanhoenacker, F., Verbruggen, L. et al. (2000). Mutations in the gene encoding the latency-associated peptide of TGF-beta 1 cause Camurati-Engelmann disease. *Nat. Genet.* **26**, 273-275.
Janssens, K., ten Dijke, P., Ralston, S. H., Bergmann, C. and Van Hul, W. (2003). Transforming growth factor-beta 1 mutations in Camurati-Engelmann disease lead to increased signaling by altering either activation or secretion of the mutant protein. *J. Biol. Chem.* **278**, 7718-7724.
Karsenty, G. and Wagner, E. F. (2002). Reaching a genetic and molecular understanding of skeletal development. *Dev. Cell* **2**, 389-406.
Kirn-Safran, C. B., Gomes, R. R., Brown, A. J. and Carson, D. D. (2004). Heparan sulfate proteoglycans: coordinators of multiple signaling pathways during chondrogenesis. *Birth Defects Res. C* **72**, 69-88.
Kitagawa, H., Tsutsumi, K., Tone, Y. and Sugahara, K. (1997). Developmental regulation of the sulfation profile of chondroitin sulfate chains in the chicken embryo brain. *J. Biol. Chem.* **272**, 31377-31381.
Klüppel, M., Nagle, D. L., Bucan, M. and Bernstein, A. (1997). Long-range genomic rearrangements upstream of Kit dysregulate the developmental pattern of Kit expression in W^{57} and W^{bd} mice and interfere with distinct steps in melanocyte development. *Development* **124**, 65-77.
Klüppel, M., Hoodless, P. A., Wrana, J. L. and Attisano, L. (2000). Mechanisms and biology of signalling by serine/threonine kinase receptors for the TGFβ superfamily. In *Frontiers in Molecular Biology: Protein Kinase Functions*. Vol. 29 (ed. J. Woodgett), pp. 303-340. Oxford: Oxford University Press.
Klüppel, M., Vallis, K. A. and Wrana, J. L. (2002). A high-throughput induction gene trap approach defines C4ST as a target of BMP signaling. *Mech. Dev.* **118**, 77-89.
Koziel, L., Kunath, M., Kelly, O. G. and Vortkamp, A. (2004). Ext1-dependent heparan sulfate regulates the range of Ihh signaling during endochondral ossification. *Dev. Cell* **6**, 801-813.
Kresse, H. and Schonherr, E. (2001). Proteoglycans of the extracellular matrix and growth control. *J. Cell Physiol.* **189**, 266-274.
Kusche-Gullberg, M. and Kjellen, L. (2003). Sulfotransferases in glycosaminoglycan biosynthesis. *Curr. Opin. Struct. Biol.* **13**, 605-611.
Martel-Pelletier, J. (2004). Pathophysiology of osteoarthritis. *Osteoarthr. Cartilage* **12**, S31-S33.
Massague, J. (2000). How cells read TGF-beta signals. *Nat. Rev. Mol. Cell Biol.* **1**, 169-178.
McLeod, M. J. (1980). Differential staining of cartilage and bone in whole mouse fetuses by alcian blue and alizarin red S. *Teratology* **22**, 299-301.
Merry, C. L. and Wilson, V. A. (2002). Role of heparan sulfate-2-O-sulfotransferase in the mouse. *Biochim. Biophys. Acta* **1573**, 319-327.
Minina, E., Kreschel, C., Naski, M. C., Ornitz, D. M. and Vortkamp, A. (2002). Interaction of FGF, Ihh/Pthlh, and BMP signaling integrates chondrocyte proliferation and hypertrophic differentiation. *Dev. Cell* **3**, 439-449.
Miyazono, K., Maeda, S. and Imamura, T. (2004). Coordinate regulation of cell growth and differentiation by TGF-beta superfamily and Runx proteins. *Oncogene* **23**, 4232-4237.
Nagy, A. and Rossant, J. (1993). Production of completely ES cell-derived fetuses. In *Gene Targeting: A Practical Approach* (ed. A. L. Joyner), pp. 147-179. Oxford: Oxford University Press.
Nybakken, K. and Perrimon, N. (2002). Heparan sulfate proteoglycan modulation of developmental signaling in Drosophila. *Biochim. Biophys. Acta* **1573**, 280-291.
Okuda, T., Mita, S., Yamauchi, S., Matsubara, T., Yagi, F., Yamamori, D., Fukuta, M., Kuroiwa, A., Matsuda, Y. and Habuchi, O. (2000). Molecular cloning, expression, and chromosomal mapping of human chondroitin 4-sulfotransferase, whose expression pattern in human tissues is different from that of chondroitin 6-sulfotransferase. *J. Biochem.* **128**, 763-770.
Perrimon, N. and Hacker, U. (2004). Wingless, hedgehog and heparan sulfate proteoglycans. *Development* **131**, 2509-2511; author reply 2511-2513.
Rossi, A., Bonaventure, J., Delezoide, A. L., Cetta, G. and Superti-Furga, A. (1996). Undersulfation of proteoglycans synthesized by chondrocytes from a patient with achondrogenesis type 1B homozygous for an L483P substitution in the diastrophic dysplasia sulfate transporter. *J. Biol. Chem.* **271**, 18456-18464.
Rountree, R. B., Schoor, M., Chen, H., Marks, M. E., Harley, V., Mishina, Y. and Kingsley, D. M. (2004). BMP receptor signaling is required for postnatal maintenance of articular cartilage. *PLoS Biol.* **2**, e355.
Saito, T., Kinoshita, A., Yoshiura, K., Makita, Y., Wakui, K., Honke, K., Niikawa, N. and Taniguchi, N. (2001). Domain-specific mutations of a transforming growth factor (TGF)-beta 1 latency-associated peptide cause Camurati-Engelmann disease because of the formation of a constitutively active form of TGF-beta 1. *J. Biol. Chem.* **276**, 11469-11472.
Sanford, L. P., Ormsby, I., Gittenberger-de Groot, A. C., Sariola, H., Friedman, R., Boivin, G. P., Cardell, E. L. and Doetschman, T. (1997). TGFbeta2 knockout mice have multiple developmental defects that are non-overlapping with other TGFbeta knockout phenotypes. *Development* **124**, 2659-2670.
Scharstuhl, A., Glansbeek, H. L., van Beuningen, H. M., Vitters, E. L., van der Kraan, P. M. and van den Berg, W. B. (2002). Inhibition of endogenous TGF-beta during experimental osteoarthritis prevents osteophyte formation and impairs cartilage repair. *J. Immunol.* **169**, 507-514.
Scharstuhl, A., Vitters, E. L., van der Kraan, P. M. and van den Berg, W. B. (2003). Reduction of osteophyte formation and synovial thickening by adenoviral overexpression of transforming growth factor beta/bone morphogenetic protein inhibitors during experimental osteoarthritis. *Arthritis Rheum.* **48**, 3442-3451.
Selleck, S. B. (2000). Proteoglycans and pattern formation. *Trends Genet.* **16**, 206-212.
Serra, R. and Chang, C. (2003). TGF-beta signaling in human skeletal and patterning disorders. *Birth Defects Res. C* **69**, 333-351.
Serra, R., Karaplis, A. and Sohn, P. (1999). Parathyroid hormone-related peptide (PTHrP)-dependent and -independent effects of transforming growth factor beta (TGF-beta) on endochondral bone formation. *J. Cell Biol.* **145**, 783-794.
Shum, L., Coleman, C. M., Hatakeyama, Y. and Tuan, R. S. (2003). Morphogenesis and dysmorphogenesis of the appendicular skeleton. *Birth Defects Res. C* **69**, 102-122.
Shworak, N. W., HajMohammadi, S., de Agostini, A. I. and Rosenberg, R. D. (2002). Mice deficient in heparan sulfate 3-O-sulfotransferase-1: normal hemostasis with unexpected perinatal phenotypes. *Glycoconjugate J.* **19**, 355-361.
Sugahara, K. and Kitagawa, H. (2000). Recent advances in the study of the biosynthesis and functions of sulfated glycosaminoglycans. *Curr. Opin. Struct. Biol.* **10**, 518-527.
ten Dijke, P. and Hill, C. S. (2004). New insights into TGF-beta-Smad signalling. *Trends Biochem. Sci.* **29**, 265-273.
Theocharis, A. D., Vynios, D. H., Papageorgakopoulou, N., Skandalis, S. S. and Theocharis, D. A. (2003). Altered content composition and structure of glycosaminoglycans and proteoglycans in gastric carcinoma. *Int. J. Biochem. Cell Biol.* **35**, 376-390.
Thiele, H., Sakano, M., Kitagawa, H., Sugahara, K., Rajab, A., Hohne, W., Ritter, H., Leschik, G., Nurnberg, P. and Mundlos, S. (2004). Loss of chondroitin 6-O-sulfotransferase-1 function results in severe human chondrodysplasia with progressive spinal involvement. *Proc. Natl. Acad. Sci. USA* **101**, 10155-10160.
Tsara, M. E., Theocharis, A. D. and Theocharis, D. A. (2002). Compositional and structural alterations of proteoglycans in human rectum carcinoma with special reference to versican and decorin. *Anticancer Res.* **22**, 2893-2898.

Uebelhart, D., Thonar, E. J., Delmas, P. D., Chantraine, A. and Vignon, E. (1998). Effects of oral chondroitin sulfate on the progression of knee osteoarthritis: a pilot study. *Osteoarthr. Cartilage* **6**, 39-46.

Vortkamp, A. (2001). Interaction of growth factors regulating chondrocyte differentiation in the developing embryo. *Osteoarthr. Cartilage* **9**, S109-S117.

Wilson, V. A., Gallagher, J. T. and Merry, C. L. (2002). Heparan sulfate 2-O-sulfotransferase (Hs2st) and mouse development. *Glycoconjugate J.* **19**, 347-354.

Yamauchi, S., Mita, S., Matsubara, T., Fukuta, M., Habuchi, H., Kimata, K. and Habuchi, O. (2000). Molecular cloning and expression of chondroitin 4-sulfotransferase. *J. Biol. Chem.* **275**, 8975-8981.

Yi, S. E., Daluiski, A., Pederson, R., Rosen, V. and Lyons, K. M. (2000). The type I BMP receptor BMPRIB is required for chondrogenesis in the mouse limb. *Development* **127**, 621-630.

Yoon, B. S. and Lyons, K. M. (2004). Multiple functions of BMPs in chondrogenesis. *J. Cell Biochem.* **93**, 93-103.

Development